Available online at www.sciencedirect.com
SCIENCE DIRECT
ELSEVIER
International Journal of Refrigeration 28 (2005) 840–850
REVUE INTERNATIONALE DU FROID
INTERNATIONAL JOURNAL OF
refrigeration
www.elsevier.com/locate/ijrefrig

Extension of soil thermal conductivity models to frozen meats with low and high fat content

V.R. Tarnawski[a,*], D.J. Cleland[b], S. Corasaniti[c], F. Gori[d], R.H. Mascheroni[e]

[a]*Division of Engineering, Saint Mary's University 923 Robie St, Halifax, Canada B3H 3C3*
[b]*Institute of Technology and Engineering, Massey University Palmerston, New Zealand*
[c]*Department of Mechanical Engineering, University of Rome 'Tor Vergata' 00133 Roma, Italy*
[d]*Department of Mechanical Engineering, University of Rome 'Tor Vergata' 00133 Roma, Italy*
[e]*CIDCA and Departamento Ingeniería Química, Facultad de Ingeniería, UNLP_47 y 116 (1900) La Plata, Argentina.*

Received 24 November 2003; received in revised form 12 January 2005; accepted 31 January 2005
Available online 2 April 2005

Abstract

Thermal conductivity models of frozen soils were analyzed and compared with similar models developed for frozen foods. In total, eight thermal conductivity models and 54 model versions were tested against experimental data of 13 meat products in the temperature range from 0 to −40 °C. The model by deVries, with water + ice (*wi*) as the continuous phase, showed overall the best predictions. The use of *wi* leads generally to improved predictions in comparison to *ice*; *water* as the continuous phase is beneficial only to deVries model, mostly from −1 to −20 °C; *fat* is advantageous only to meats with high fat content. The results of this work suggest that the more sophisticated way of estimating the thermal conductivity for a disperse phase in the deVries model might be more appropriate than the use of basic multi-phase models (geometric mean, parallel, and series). Overall, relatively small differences in predictions were observed between the best model versions by *deVries*, *Levy*, *Mascheroni*, *Maxwell* or *Gori* as applied to frozen meats with low content of fat. These differences could also be generated by uncertainty in meat composition, temperature dependence of thermal conductivity of ice, measurement errors, and limitation of predictive models.

Keywords: Frozen food; Modelling; Thermal conductivity; Experiment; Comparison; Soil

Modèles de la conductivité thermique du sol appliqués aux viandes surgelées à faible et à forte teneur en matière grasse

Mots clés : Produit congelé ; Modélisation ; Conductivité thermique ; Expérimentation ; Comparaison ; Sol

1. Introduction

Soils and foods are both heterogeneous porous media and share some similar features as well as a number of differences. Soils are mixtures of inorganic loose particles of

* Corresponding author.
E-mail address: vlodek.tarnawski@smu.ca (V.R. Tarnawski).

0140-7007/$35.00
doi:10.1016/j.ijrefrig.2005.01.012

Nomenclature

a, b, c	axes of ellipsoidal food components
a_0, a_1, a_2	constants in Eqs. (20) and (21)
F	alternative function for θ_d used in Levy's model
f	fat as continuous phase
f-d_{GMM}	fat as continuous phase; λ of dispersed phase (d) evaluated by GMM (Eq. (3a))
f-$d_{\|}$	fat as continuous phase; λ of dispersed phase (d) evaluated by $\|$ (Eq. (1))
f-$d_{\sum}$	fat as continuous phase; λ of dispersed phase (d) evaluated by $\sum$ (Eq. (2))
fib_{GMM}	λ_{fiber} (models by Mascheroni)–evaluated by GMM (Eq. (3a))
$fib_{\|}$	λ_{fiber} (models by Mascheroni)–evaluated by $\|$ (Eq. (1))
$fib_{\sum}$	λ_{fiber} (models by Mascheroni)–evaluated by $\sum$ (Eq. (2))
g	shape factor
k	weighting factor
i	ice as continuous phase
i-d_{GMM}	ice as continuous phase; λ of dispersed phase (d) evaluated by GMM (Eq. (3a))
i-$d_{\|}$	ice as continuous phase; λ of dispersed phase (d) evaluated by $\|$ (Eq. (1))
i-$d_{\sum}$	ice as continuous phase; λ of dispersed phase (d) evaluated by $\sum$ (Eq. (2))
M	mass fraction
N	the number of solid components
n	number of phases, data records, etc.
p	ellipsoid shape value (equatorial diameter/-distance between ellipsoid poles)
RMSE	root mean square error
s_{GMM}	solids λ evaluated by GMM (Eq. (3a))
T	temperature (°C)
w	water as continuous phase
wi	water + ice as continuous phase
wi_{GMM}	water + ice = continuous phase; λ evaluated by GMM (Eq. (3a))
$wi_{\|}$	water + ice = continuous phase; λ evaluated by $\|$ model (Eq. (1))
$wi_{\sum}$	water + ice = continuous phase; λ evaluated by $\sum$ (Eq. (2))

Greek

β	variable in Eqs. (13) and (14)
θ	volume fraction
λ	thermal conductivity (W/m °C)
ρ	density
δ	λ_d/λ_{con}
σ	variable in Eqs. (7) and (8)
ξ	variable in Eqs. (15) and (16)

Subscripts

a	air
ash	ash/mineral
b	bulk
bw	bound water
car	carbohydrate
con	continuous phase
d	dispersed phase
exp	experimental
f	initial freezing point
fat	fat
fib	meat-fibre
GMM	geometric mean model
ice	ice
j	food component number
prot	proteins
s	solids
un	unfrozen water
w	water
wi	water + ice
$\|$	heat flow $\|$ to fibers of meat
$\perp$	heat flow $\perp$ to fibers of meat

various sizes and shapes, organic matter, water, and air. The total volume fraction of water and air is known as the soil porosity. Foods are heterogeneous capillary-porous colloidal materials composed of numerous solid constituents, such as carbohydrates, fats, proteins, vitamins and minerals, plus water; air voids can also be present. In the food literature, porosity generally refers to the air component only. Porosity of soils (relative volume of air plus water) typically varies from 30 to 60% while for foods moisture content generally varies from 15 to 90%. The water, containing dissolved substances, is a major component in both soils and foods and its transition from liquid into ice is the greatest factor influencing change in thermal properties with temperature (T). In soils, water exists in gravitational, capillary, and hygroscopic (bound) forms, while foods contain only capillary and bound water. Foods are generally saturated with water, while soils experience great variation of water content, from dryness to a field capacity (volumetric water content at saturation minus the gravitational water). A large part of the water, in both soils and foods, freezes rapidly between 0 and −5 °C, therefore, very sparse thermal conductivity (λ) data is available in this T range. Excluding water, ice and air, the thermal conductivity of other food components are similar, while in soils the thermal conductivity of quartz is large compared with other mineralogical constituents. Soil composition is usually given by volumetric fractions, while for foods mass fraction is most commonly employed.

Analysis, design and simulation of food freezing and

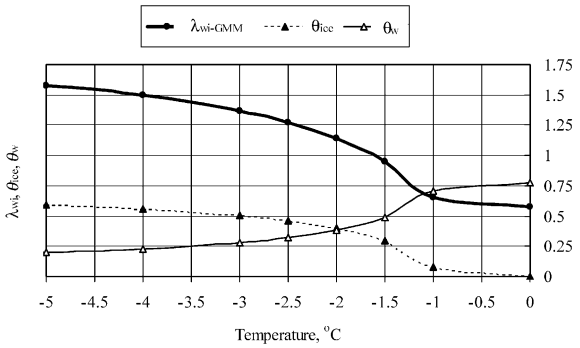

Fig. 1. Volumetric content of ice (θ_{ice}), water (θ_w) and $\lambda_{wi\text{-}GMM}$ vs. T for leg-muscle-parallel.

storage process demands reliable and easily accessible thermal property data across a wide range of temperatures, particularly below the freezing point. The λ of frozen foods is a key property to the above applications. In general, experimental determination of λ is difficult, time and labour expensive, and error prone. Therefore, estimation of λ from predictive models, based on food composition, is often employed. A similar modelling approach has also been used in soils. Apart from the basic series and parallel models and combination of these, the most commonly quoted thermal conductivity models in the frozen food literature are the Maxwell–Eucken equation [1], Levy's modification to the Maxwell–Eucken equation [2] and the effective medium theory (EMT) [3]. Mascheroni et al. [4] proposed a model for frozen meat which was verified against a limited set of experimental data only. Pham [5] found Levy's model the most accurate of seven models (the model by Mascheroni was not considered) tested for meats with low and high fat content. Models developed for soil systems that could be extended to frozen foods, include: the weighted average by deVries [6], a cubic cell by Gori [7], self-consistent approximation by Sundberg [8], and geometric mean by Lichtenecker [9]. The existing literature shows lack of clear evidence of the application of frozen soil models to frozen foods.

2. Scope of the paper

The purpose of this paper is to evaluate the application of frozen soil models to food systems and compare them with the best frozen food models under assumption that thermal conductivity of food components is not dependent on T. The λ models developed from the original Maxwell relationship (Maxwell–Eucken, Levy, deVries) require component information regarding the continuous (*con*) and dispersed phases (*d*). Commonly, the dominant volumetric fraction of food component (usually water or ice) is assumed as the continuous medium. This assumption, however, may not be entirely true, as at the beginning of freezing, the unfrozen water content can still be a dominant phase, i.e. larger than newly formed ice fraction (Fig. 1). In addition, changing the continuous phase from water into ice leads to a discontinuity problem, i.e. a step change of λ as the $\lambda_{ice} > 4\lambda_w$. These problems, might be eliminated if water and ice are treated as one continuous phase (*wi*) whose lumped conductivity λ_{wi} changes smoothly over the entire freezing T range, i.e. from λ_w (unfrozen foods) to λ_{ice} (fully frozen foods)—Fig. 1. The lumped λ_{wi} and λ_d can be evaluated by one of the simple multi-phase models such as geometric mean, parallel and series. Therefore, another objective of this paper is to examine the influence of the continuous phase selection (*water, ice, water+ice, fat*) on the effective thermal conductivity of frozen foods.

3. Review of predictive models for foods and soils

3.1. Basic multi-phase models

The majority of the above models require additional data regarding the lumped thermal conductivity of the continuous and dispersed phases. This information is usually obtained by applying parallel, series, or geometric-mean models. The parallel model ($\|$) assumes parallel configuration of the system components in the direction of heat flow:

$$\lambda = \frac{\sum_1^n \theta_j \lambda_j}{\sum_1^n \theta_j} \tag{1}$$

The series model ($\sum$) assumes series configuration of the system components in the direction of heat flow:

$$\lambda = \frac{\sum_1^n \theta_j}{\sum_1^n \frac{\theta_j}{\lambda_j}} \tag{2}$$

The geometric-mean model (GMM), proposed by Lichtenecker [9], is not based on any physical concepts, but it is commonly used due to its simplicity.

$$\lambda = \prod_1^n \lambda_j^{\theta_j} \tag{3a}$$

The results produced by the GMM model are intermediate between the $\|$ and $\sum$ model. Good predictive results of this model, for frozen saturated soils, were reported by Johansen [10] who used the following form of this model:

$$\lambda = \lambda_s^{\theta_s} \lambda_{ice}^{\theta_{ice}} \lambda_{un}^{\theta_{un}} \tag{3b}$$

This model structure can be easily applied for frozen foods because the evaluation of the lumped conductivity of solid components, λ_s, excludes the ice and other water fractions.

In general, the thermal conductivity models can be subdivided into two groups; the first group considering only

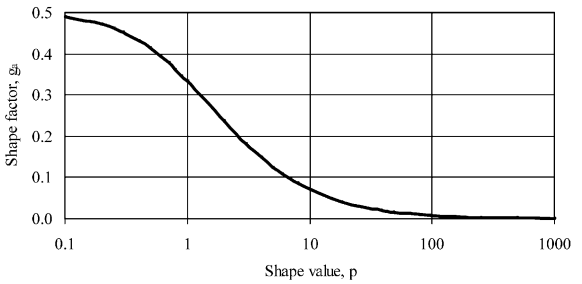

Fig. 2. Shape factor g_a as a function of the ellipsoid shape value p.

two phases, continuous and dispersed one (e.g. Maxwell–Eucken, Levy), and the second one with more than two phases (solid, liquid, gaseous).

3.2. Two-phases models

3.2.1. Maxwell–Eucken

Originally, this model was developed for predicting the electrical conductivity of non-interacting homogeneous spheres (dispersed phase) in a homogeneous continuous phase. The of this binary system ($con+d$) was given by:

$$\lambda = \lambda_{\mathrm{con}} \frac{1 + \frac{2}{\delta} + 2\theta_{\mathrm{d}}(1 - \frac{1}{\delta})}{1 + \frac{2}{\delta} - \theta_{\mathrm{d}}(1 - \frac{1}{\delta})} \tag{4}$$

where $\delta = \lambda_{\mathrm{d}}/\lambda_{\mathrm{con}}$. When applied to frozen foods, this model gives different λ values depending on which components are chosen to be a part of the continuous and dispersed phases and how the lumped λ of each phase is estimated. Eq. (4) can be converted into a weighted average form in terms of the continuous and dispersed phases [11]:

$$\lambda = \frac{k_{\mathrm{con}}\theta_{\mathrm{con}}\lambda_{\mathrm{con}} + k_{\mathrm{d}}\theta_{\mathrm{d}}\lambda_{\mathrm{d}}}{k_{\mathrm{con}}\theta_{\mathrm{con}} + k_{\mathrm{d}}\theta_{\mathrm{d}}} \tag{5}$$

$$k_{\mathrm{d}} = \frac{1}{3}\sum_{x=abc}\left[1 + g_x(\delta - 1)\right]^{-1} = \frac{3}{\delta + 2} \tag{6}$$

where, $k_{\mathrm{con}} = 1$, g_{x} is a shape factor for each dimension of particles in the dispersed phase.

For solid spheres ($a=b=c$), $g_x = 1/3$. The λ_{d} can be evaluated by one of basic multiphase models such as, $\sum$, $\|$, or GMM.

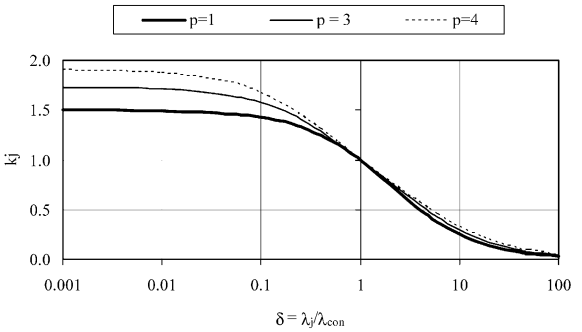

Fig. 3. Variation of k_j factor vs. $\lambda_j\lambda_{\mathrm{con}}$ for $p = 1$–3–4.

3.2.2. Levy modification to Maxwell–Eucken model

Levy [2] modified the Maxwell–Eucken model (Eq. (4)) by replacing the volume fraction of a dispersed phase, θ_{d}, by a function F so that the predictions are independent of the designation of phases as continuous or dispersed:

$$F = \frac{1}{\sigma} - \frac{1}{2} + \theta_{\mathrm{d}} - \frac{1}{2}\sqrt{\left(\frac{2}{\sigma} - 1 + 2\theta_{\mathrm{d}}\right)^2 - 8\frac{\theta_{\mathrm{d}}}{\sigma}} \tag{7}$$

$$\sigma = \frac{(\delta - 1)^2}{(\delta + 1)^2 + 0.5\delta} \tag{8}$$

3.3. Multi-phases models

3.3.1. deVries model

Fricke [12] was the first to consider extension of the Maxwell's model to homogeneous ellipsoidal particles. Later on, the same idea was used by de Vries [6] for predicting λ of moist soils; i.e. a spherical shape of solid grains was replaced with rotated oblate ellipsoids dispersed in the continuous medium (water, air).

$$\lambda = \frac{k_{\mathrm{con}}\theta_{\mathrm{con}}\lambda_{\mathrm{con}} + \sum_1^N k_j\theta_j\lambda_j}{k_{\mathrm{con}}\theta_{\mathrm{con}} + \sum_1^N k_j\theta_j} \tag{9}$$

where N is the number of solid components; each solid grain of component (j) has the same weighting factor k_j and the same thermal conductivity λ_j.

If the axes (a, b, c) of ellipsoidal granules are oriented randomly, k_j can be obtained from

$$k_j = \frac{1}{3}\sum_{x=abc}\left[1 + (\frac{\lambda_j}{\lambda_{\mathrm{con}}} - 1)g_x\right]^{-1} = \frac{(\nabla T)_j}{(\nabla T)_{\mathrm{con}}} \tag{10}$$

According to de Vries [6] k_j represents the ratio of the average T gradient in a solid constituent (j) to the average T gradient in the continuous phase. In practice, k_j is an adjustment factor improving λ predictions. Eq. (10) converts to unity ($k_{\mathrm{con}} = 1$) if the j constituent is assumed as the continuous phase ($\lambda_j = \lambda_{\mathrm{con}}$). For the dispersed phase, the k_j depends on $\lambda_j/\lambda_{\mathrm{con}}$ and a solid particle ellipsoidal shape factor for each of three axes ($g_{x=a,b,c}$). The shape factors g_a, g_b, and g_c depend on ratios of the ellipsoid axes a, b, and c. The sum of g_a, g_b, and g_c is unity. For rotated ellipsoids ($a = b$), $g_a = g_b$, $g_c = 1 - 2g_a$. The g_a values can be estimated from equations given by Carslaw and Jaeger [13]: oblate ellipsoids: $p = a/c > 1$

$$g_a = \frac{p^2}{2\sqrt{(p^2 - 1)^3}}\left[\frac{\pi}{2} - \arctan(\frac{1}{\sqrt{p^2 - 1}}) - \frac{\sqrt{p^2 - 1}}{p^2}\right] \tag{11}$$

prolate ellipsoids: $p = a/c < 1$

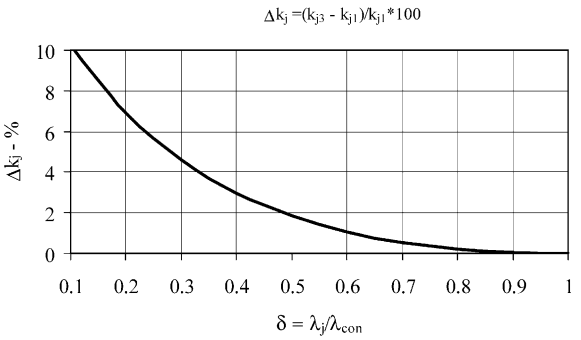

Fig. 4. Relative Δk_j change with δ (oblate ellipsoid, $p=3$ wrt. sphere, $p=1$).

$$g_a = 0.5\left[\frac{1}{1-p^2} - \frac{p^2}{2\sqrt{(1-p^2)^3}}\ln\left(\frac{1+\sqrt{1-p^2}}{1-\sqrt{1-p^2}}\right)\right] \tag{12}$$

Variation of the shape factor g_a as a function of a shape value p is shown on Fig. 2. Examples of the k_j values, for rotated ellipsoids ($p=3$ and 4) and for a sphere ($p=1$) vs. the ratio λ_j/λ_{con}, are shown in Fig. 3. The model is simple to use when applied to saturated porous media. It requires, however, knowledge regarding the shape of solid grains, which can vary from oblate to prolate ellipsoids, thus including also a sphere. For a system made of spherical solids ($a=b=c$; $g_a=g_b=g_c=1/3$), Eq. (9) reduces to a form very similar in appearance to the Maxwell's model (Eq. (5)). When both models (Eqs. (5) and (9)) are to be applied to frozen foods, it is important to be aware of some hidden disparities. First, it is more likely that solid components resemble the shape of oblate ellipsoids ($p>1$) rather then perfect spheres ($p=1$). Secondly, Eq. (5) treats the dispersed components as a single phase, while Eq. (9) handles each dispersed component individually. The spherical weighting factor k_d depends on δ only, while k_j depends on the δ and also on the shape value p of each individual component of the dispersed phase. For foods, δ varies approximately from 0.1 to 0.3 and the use of p values for oblate ellipsoids rather than sphere (e.g. $p=3$) leads to relative change in k_j ranging from 5 to 10% (Fig. 4). Furthermore, in Eq. (5), λ_d is evaluated by one of simple multi-phase models (Eqs. (1)–(3)), while individual λ_j values are used in Eq. (9).

3.3.2. Gori's model

The model assumes a cubic cell of lumped solids surrounded by another cubic cell composed of unfrozen water and ice as the continuous medium. For foods, the model was converted from a three phase system (solids, water, ice) into a two phase system consisting of food solids as a dispersed phase and *wi* as the continuous phase. The first model considers the horizontal parallel isotherms (*hpi-wi*) in the cubic cell.

$$\frac{1}{\lambda} = \frac{\beta-1}{\lambda_{wi}\beta} + \frac{\beta}{\lambda_{wi}[\beta^2-1]+\lambda_s} \tag{13}$$

The second model takes into account a vertical parallel heat flux (*vphf-wi*) in the cubic cell.

$$\lambda = \frac{1}{\frac{\beta(\beta-1)}{\lambda_{wi}} + \frac{\beta}{\lambda_s}} + \lambda_{wi}\frac{\beta^2-1}{\beta^2}, \quad \beta = \sqrt[3]{\frac{1}{1-\theta_w-\theta_a}} \tag{14}$$

3.3.3. Mascheroni's model

The model was developed for solid frozen meats with the following assumptions: water in fibres was treated as a randomly dispersed phase in a continuous matrix of the remaining food tissue; partially dehydrated fibres were surrounded by ice; at $T>T_f$ all the water was within the fibre; and, at $T<T_f$ ice was being formed in the extra cellular space at expense of water in the fibres. One model option considers that heat flow is perpendicular ($\perp$) to the meat fibres:

$$\lambda_\perp = \frac{\lambda_{ice}\lambda_{fib}(1-\xi_{ice})}{\xi_{ice}\lambda_{fib}+\lambda_{ice}(1-\xi_{ice})} + \lambda_{ice}\xi_{ice} \tag{15}$$

The other model option is based on assumption that heat flow is parallel ($\|$) to the meat fibers:

$$\lambda_\| = \lambda_{ice}\xi_{ice} + (1-\xi_{ice}) \times\left\{\lambda_{ice}\xi_{ice}^2 + \lambda_{fib}(1-\xi_{ice})^2 + \frac{4\xi_{ice}(1-\xi_{ice})}{\frac{1}{\lambda_{fib}}+\frac{1}{\lambda_i}}\right\} \tag{16}$$

where $\xi_{ice} = 1-\sqrt{1-\theta_{ice}}$. Originally, the thermal conductivity of meat fibers, λ_{fib}, was evaluated by the Maxwell–Eucken model using the fiber component composition. In this paper, however, the λ_{fib} is modeled by simple multi-phase models (GMM, $\|$, $\sum$).

3.3.4. Self-consistent approximation (SCA)–effective medium theory (EMT) model

The SCA model was originally developed by Bruggeman [14] for predicting λ of a mixture of isotropic materials. Later on, the same expression was utilized by Landeauer [15] as the effective medium theory (EMT) model and used for evaluating the electrical resistance of binary metallic mixtures. Then, the model was adapted to predicting the λ of vegetable foods [3].

$$\sum_1^n \theta_j \frac{\lambda_j-\lambda}{\lambda_j+2\lambda} = 0 \tag{17}$$

Sundberg [8] used the same model, a slightly different form, for predicting λ of soils.

$$\lambda = \frac{1}{3}\frac{1}{\sum_1^3 \frac{\theta_j}{\lambda_j+2\lambda}} \tag{18}$$

In both forms (Eqs. (17) and (18)), θ_j and λ_j are the volume fraction and thermal conductivity of the j component,

Table 1
Mass composition of the meats under investigation

Food	Code #	M_w	M_{prot}	M_{fat}	M_{ash}	M_{car}
Leg muscle ‖	1	0.736	0.199	0.047	0.011	0.007
Leg muscle minced	2	0.739	0.186	0.045	0.01	0.02
Hearts	3	0.698	0.15	0.123	0.012	0.017
Hearts minced	4	0.688	0.149	0.139	0.01	0.014
Livers	5	0.689	0.194	0.062	0.015	0.04
Livers minced	6	0.677	0.208	0.037	0.02	0.058
Brains	7	0.79	0.103	0.076	0.014	0.017
Kidneys	8	0.799	0.145	0.031	0.013	0.012
Thymus	9	0.7919	0.143	0.064	0.001	0.0001
Thymus minced	10	0.7589	0.135	0.092	0.014	0.0001
Leg muscle ⊥	11	0.725	0.193	0.072	0.009	0.001
Fat	12	0.1329	0.032	0.834	0.001	0.0001
Fat minced	13	0.1109	0.029	0.858	0.002	0.0001

Note. The M_{car} have been causing a calculation problem in the model by Mascheroni, therefore, instead of 0 a very small number 0.0001 was assigned, at expense of M_w.

respectively. If the system is composed of more than two phases, both equations have an implicit form and must be solved by an iterative method. In fact, frozen foods and soils are examples of three-phase systems, i.e. consisting of unfrozen water, ice and solids.

$$\lambda_1 = \lambda_w \quad \theta_1 = \theta_{un} \quad \lambda_2 = \lambda_{ice} \quad \theta_2 = \theta_{ice}$$

$$\lambda_3 = \lambda_s \quad \theta_3 = 1 - \theta_w - \theta_a$$

3.3.5. Modified resistor series model

Cleland [16] proposed a modified resistor series model applied to calculating λ of frozen foods.

$$\frac{\theta_w + \theta_{bw} + \theta_s}{\lambda} = \frac{\theta_w + \theta_{bw}}{\lambda_w} + \frac{\theta_s}{\sum_{j=1}^{n} \frac{\theta_j}{\theta_s} \lambda_j} \tag{19}$$

4. Experimental data and model testing

The reviewed models were tested against the experimental λ data in the T range 0 to −40 °C for 13 meats with low and high fat content (Table 1) published by Pham and Willix [17]. The food component mass fractions in this data set do not always sum exactly to 1. When the mass fractions were smaller than 1, then the remainder was arbitrarily assigned to carbohydrates. If there was a surplus, then all the component mass fractions were proportionally reduced. None of the products contained significant air voids. The experimental data covers only a few points for each product, which restricts comparison with the predictive models. Therefore, instead of the real experimental data, the following empirical equations, developed by Pham and Willix [17] were used.

$$T > T_f \quad \lambda = \lambda_f + a_0(T - T_f) \tag{20}$$

$$T < T_f \quad \lambda = \lambda_f + a_1(T - T_f) + a_2\left(\frac{1}{T} - \frac{1}{T_f}\right) \tag{21}$$

The fitted parameters are given in Table 2. The thermal conductivity and density data for the food product components used to make predictions was assumed to be T independent and their values (Table 3) were given by Choi and Okos [18].

The mass fraction of unfrozen water (including bound water) was estimated from:

$$M_{un} = M_w - M_{ice} \tag{22}$$

In the frozen range, the mass fraction of ice content was estimated from the widely used empirical relationship, developed by Schwartzberg [19], which is based on Raoult's law of dilute solutions and the Claussius–Clapeyron relationship:

$$M_{ice} = (M_w - M_{bw})\left(1 - \frac{T_f}{T}\right) \tag{23}$$

The freezing point and bound water mass fractions were based on the data and relationships given by Pham and Willix [17]:

$$T_f = -0.9\ ^{\circ}\mathrm{C} \quad M_{bw} = 0.4 M_{prot} \tag{24}$$

The mass fractions of all components were converted to volumetric fractions.

$$\theta_j = M_j \frac{\rho_b(T)}{\rho_j} \tag{25}$$

The bulk density of frozen food $\rho_b(T)$ for $T < T_f$ can be obtained from:

$$\rho_b(T) = \frac{1}{\sum_{j=1}^{n} \frac{M_j}{\rho_j}} \tag{26}$$

Table 4 gives the volumetric composition of the unfrozen

Table 2
Fitted parameters for Eq. (21) by Pham and Willix (1989)

Product	λ_f	a_0	a_1	a_2	Product	λ_f	a_0	a_1	a_2
Leg muscle ‖	0.450	0.0009	−0.0063	0.69	Kidneys	0.507	0.0012	−0.0075	0.78
Leg muscle min.	0.466	0.0011	−0.0043	0.71	Thymus	0.497	0.0012	−0.0047	0.91
Hearts	0.390	0.0009	−0.0046	0.71	Thymus min.	0.487	0.0009	−0.0053	0.85
Hearts minced	0.407	0.0008	−0.0065	0.68	Leg muscle ⊥	0.421	0.001	−0.0037	0.67
Livers	0.417	0.0006	−0.0073	0.65	Fat	0.219	−0.0005	−0.0003	0.05
Livers minced	0.425	0.0012	−0.0067	0.67	Fat minced	0.212	−0.0004	0.0000	0.06
Brains	0.494	0.0003	−0.0039	0.84					

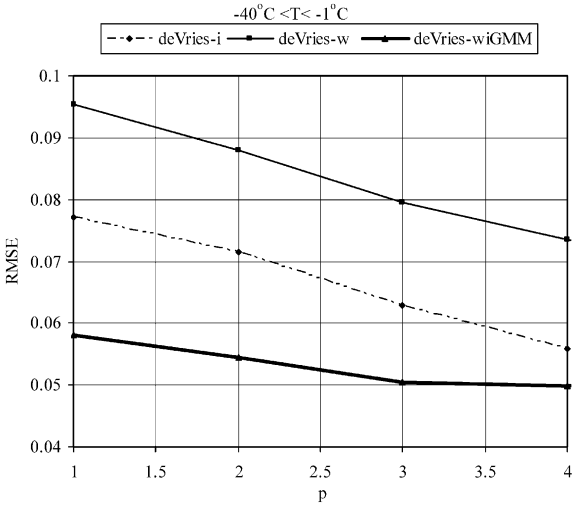

Fig. 5. Performance of deVries model vs. ellipsoids shape factor p.

products calculated from the mass fraction composition data. Table 5 shows four continuous phases used in this paper, namely: water, ice, water + ice, fat. When a phase consists of more than one component, a lumped λ was estimated from the component data using the ||, $\sum$ or GMM models as these are the simplest to apply. These three models were also used to calculate the lumped λ for the solid components (other than ice) and λ_{fib} in the model by Mascheroni [4]. In deVries model (Eq. (9)), food components were considered as rotated oblate ellipsoids whose shape values (p) were selected upon results of preliminary simulation (Fig. 5). A change from the spherical shape ($p=1$) to flattened ellipsoids ($p=2$–4) is without a doubt beneficial to the model predictions. For example, the deVries-wi model performance is improving with p increase from 1 to 3 and then it remains constant. For that reason, $p=3$ was applied to all solid components of the frozen foods (Table 6).

5. Results and discussion

The 54 versions of the eight thermal conductivity models have been analyzed and compared with the experimental data for frozen foods. The root mean square error (RMSE) was used to determine how well the predictive models fit the measured data.

$$\mathrm{RMSE} = \sqrt{\frac{1}{n}\sum_{1}^{n}\left[\frac{\lambda_{exp}-\lambda}{\lambda_{exp}}\right]^2} \tag{27}$$

The RMSE was evaluated for the 54 λ model versions and four T ranges (0 to −40 °C; −1 to −40 °C; −1 to −20 °C; −1 to −5 °C). Each version of the predictive model was assessed on a basis of data generated by that model (λ_{model}) and λ_{exp} obtained from equations by Pham and Willix [17].

Table 3
Thermal conductivity and density of food components by Choi and Okos (1986)

Component	Water	Ice	Protein	Fat	Ash	Carbohydrate
λ (W/m K)	0.56	2.21	0.20	0.18	0.33	0.20
ρ (kg/m^3)	1000	917	1380	930	2424	1600

Table 4
Volume composition of the unfrozen meats under investigation

Food	Code #	ρ_b	θ_w	θ_{prot}	θ_{fat}	θ_{ash}	θ_{car}
Leg muscle ‖	1	1055.5	0.779	0.158	0.054	0.005	0.005
Leg muscle minced	2	1056.8	0.783	0.148	0.051	0.004	0.013
Hearts	3	1040.3	0.728	0.117	0.138	0.005	0.011
Hearts minced	4	1036.2	0.715	0.116	0.156	0.004	0.009
Livers	5	1069.5	0.739	0.156	0.072	0.007	0.027
Livers minced	6	1087.2	0.738	0.170	0.043	0.009	0.039
Brains	7	1032.8	0.818	0.080	0.085	0.006	0.011
Kidneys	8	1045.3	0.838	0.114	0.035	0.006	0.008
Thymus	9	1029.5	0.818	0.111	0.071	0.000	0.000
Thymus minced	10	1033.3	0.786	0.105	0.103	0.006	0.000
Leg muscle ⊥	11	1047.9	0.762	0.152	0.082	0.004	0.001
Fat	12	944.4	0.126	0.023	0.851	0.000	0.000
Fat minced	13	942.6	0.105	0.021	0.874	0.001	0.000

For T range from −1 to −5 °C, the T increment was −0.5 °C, and −2.5 °C, from −5 to −40 °C.

Tables 7–9 summarize the average RMSE for the best 10 model versions applied to 11 low fat meats (high water content), two high fat meats (low water content) and all 13 meats under investigation, respectively. As far as the λ of lean meats (11 foods with high water content) is concerned, *Masch-⊥-fib*$_{\|}$, *deVries-wi*$_{GMM}$ and *de Vries-w* model offer clearly the best predictions in T range from −1 to −5 °C and −1 to −20 °C. Slightly less accurate predictions in these two T ranges are given by *Gori-vphf-wi* and *Maxwell-wi*$_{GMM}$ (Fig. 6). In the T range from −1 to −40 °C), *deVries-wi*$_{GMM}$ produces the best predictions followed by *deVries-i* and then by a large group of models (*Maxwell-wi*$_{GMM}$, *Gori-vphf-wi*, *Masch-‖-fib*$_{GMM}$, *Masch-‖-fib*$_{\sum}$, *ETM-s*$_{GMM}$, *deVries-w*), whose performance is more or less at the same level. The predictive performance of the *Vries-w* and the *Masch-⊥-fib*$_{\|}$ model, however, is declining for T ranging from −20 to −40 °C, i.e. when a large majority of water has been converted into the ice. The *Masch-‖-fib*$_{GMM}$ and *Maxwell-wi*$_{GMM}$ predict well in all three ranges of freezing T. The *Levy-wi*$_{\|}$ model performs better than *Levy-i-d*$_{GMM}$ and offers acceptable performance in ΔT range from −1 to −20 °C and −1 to −40 °C (8 and 9th place, respectively), but it largely over-predicts the data near the freezing point (−1 to −5 °C). The *EMT-s*$_{GMM}$ and *Gori-vphf-wi* models are simple in form and provide good λ estimates for frozen and unfrozen foods. The model by Cleland [16] gives acceptable performance (10th place) in the full range of freezing T only. With regard to high fat meats (two foods with very low water content), *Levy-wi*$_{\|}$, *deVries-w* and a wide variety of Levy model versions show the best predictions in T range from −1 to −5 °C and −1 to −20 °C. For the full range of freezing T (−1 to −40 °C), *Levy-f-d*$_{\|}$, *Levy-wi*$_{\|}$, *deVries-w*, and *Levy-i-d*$_{\|}$ have the best predictions with very small differences between them. For

Table 5
Options for continuous and dispersed phases in frozen foods

Continuous phase (*con*)	Dispersed phase (*d*)
Ice (*i*)	Food solid components + water
Water + ice (*wi*)	Food solid components
Water (*w*)	Food solid components + ice
Fat (*f*)	Food solid components + ice + water

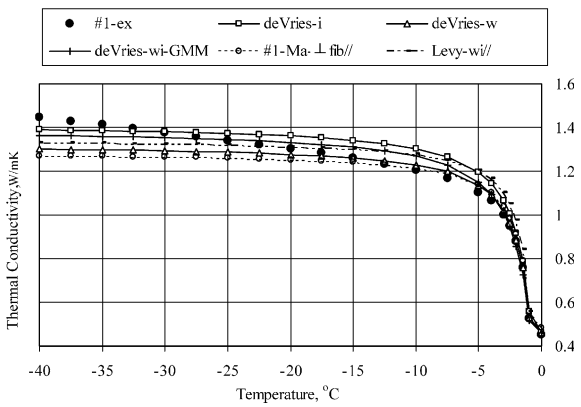

Fig. 6. The experimental λ vs. predictive data (frozen lamb leg muscle parallel).

Table 6
Shape factors for food components

Meat components	Water	Protein	Fat	Ash	Carb-hyd	Ice
Shape value (p)	100	3	3	3	3	3
Shape factor (g)	0.01	0.18	0.18	0.18	0.18	0.18

Table 7
Best predictive models—low fat meats (1–11)

0 °C	RMSE	⟨−1 °C…−5 °C⟩	RMSE	⟨−1 °C…−20 °C⟩	RMSE	⟨−1 °C…−40 °C⟩	RMSE
GeoMean-s_{GMM}	0.041	Masch-$\perp$-$fib_{\parallel}$	0.047	Masch-$\perp$-$fib_{\parallel}$	0.048	deVries-wi_{GMM}	0.050
Levy-w	0.046	deVries-w	0.048	Gori-vphf-wi	0.051	deVries-i	0.058
Levy-f-d_{GMM}	0.046	deVries-wi_{GMM}	0.048	deVries-wib_{GMM}	0.047	Maxwell-wi_{GMM}	0.058
EMT-s_{GMM}	0.047	Maxwell-wi_{GMM}	0.052	deVries-w	0.052	Gori-vphf-wi	0.058
deVries-w	0.048	Masch-$\perp$-fib_{GMM}	0.057	deVries-i	0.060	Masch-$\parallel$-fib_{GMM}	0.058
Gori-vphf-w	0.048	EMT-s_{GMM}	0.058	Masch-$\parallel$-fi_{GMM}	0.063	Masch-$\parallel$-$fib_{\sum}$	0.059
Maxwell-f-d_{GMM}	0.050	deVries-i	0.059	Maxwell-wi_{GMM}	0.064	EMT-s_{GMM}	0.061
deVries-f	0.050	Masch-$\parallel$-fib_{GMM}	0.061	Levy-$wi_{\parallel}$	0.064	deVries-w	0.061
Maxwell-w	0.050	Gori-vphf-wi	0.061	Masch-$\parallel$-$fib_{\sum}$	0.066	Levy-$wi_{\parallel}$	0.070
Masch-$\perp$-fib_{GMM}	0.050	Masch-$\parallel$-$fib_{\sum}$	0.067	EMT-s_{GMM}	0.067	Cleland	0.071

Table 8
Best predictive models—high fat meats (12–13)

0 °C	RMSE	⟨−1 °C…−5 °C⟩	RMSE	⟨−1 °C…−20 °C⟩	RMSE	⟨−1 °C…−40 °C⟩	RMSE
deVries-w	0.003	Levy-wi-$d_{\parallel}$	0.028	Levy-wi-$d_{\parallel}$	0.032	Levy-f-$d_{\parallel}$	0.031
deVries-f	0.004	deVries-w	0.029	de Vries-w	0.032	Levy-$wi_{\parallel}$	0.034
Gori-vphf-w	0.004	Levy-f-$d_{\parallel}$	0.033	Levy-f-$d_{\parallel}$	0.036	deVries-w	0.036
Levy-f-$d_{\parallel}$	0.005	Levy-wi_{GMM}	0.036	Levy-i-$d_{\parallel}$	0.039	Levy-i-$d_{\parallel}$	0.037
Maxwell-w	0.006	Maxwell-$wi_{\sum}$	0.037	Levy-wi_{GMM}	0.040	deVries-f	0.046
Gori-hpi-w	0.008	deVries-$wi_{\sum}$	0.038	deVries-$wi_{\sum}$	0.047	Levy-wi_{GMM}	0.046
Maxwell-f-$d_{\parallel}$	0.012	Levy-i-$d_{\parallel}$	0.041	Levy-i-d_{GMM}	0.049	Levy-i_{GMM}	0.053
Levy-w	0.015	Levy-i-d_{GMM}	0.048	Levy-f-d_{GMM}	0.055	deVries-$wi_{\sum}$	0.060
Levy-f-d_{GMM}	0.026	Levy-f-d_{GMM}	0.051	Levy-i-$d_{\sum}$	0.065	Levy-f-d_{GMM}	0.064
EMT-s_{GMM}	0.027	deVries-f	0.060	Levy-$wi_{\sum}$	0.069	Levy-i-$d_{\sum}$	0.071

all meats under investigation (11 lean + 2 high fat), *deVries-wi_{GMM}*, *deVries-w* and *Levy-$wi_{\parallel}$* exhibit the best performance in all T ranges followed by *Masch-$_{\perp}$-$fib_{\parallel}$*, *Gori-vphf-wi* and *ETM-s_{GMM}*. The λ of all unfrozen meat products (0 °C) was predicted very well by a large group of models (Table 9).

6. Conclusions and recommendations

The analysis of computer simulation confirms that *deVries-wi_{GMM}* has overall the best predictions for frozen meats, while for unfrozen meats, a large majority of tested models show very accurate predictions. In general, the model by deVries has a good physical basis, requires relatively small calculation effort and has a potential for further improvement, particularly in the shape description of oblate ellipsoids. The results of this work suggest also that the more sophisticated way of estimating the λ_d for a disperse phase in the deVries model might be more appropriate than the use of basic multi-phase models (GMM, $\parallel$, $\sum$). This could also be a reason that in general the deVries model performed slightly better than the other models. It appears that the performance of predictive models, as applied to frozen foods, is strongly influenced by the choice of continuous phase. The use of *wi* has a sound physical basis as both water and ice exist practically in the full range of freezing T. The freezing process, particularly between −1 and −5 °C, is simulated better with the use of *wi* than *i* alone. For this reason, the choice of *wi* as the continuous phase leads to improved λ predictions in comparison to ice (*i*). In addition, it is also easier to assess the λ_d of the dispersed phase as the thermal conductivities of solid food components are more or less in the same range. The use of *wi* in deVries model requires, however, additional calculations for k_j, which strongly depends on

Table 9
Best predictive models—overall (1–13)

0 °C	RMSE	⟨−1 °C…−5 °C⟩	RMSE	⟨−1 °C…−20 °C⟩	RMSE	⟨−1 °C…−40 °C⟩	RMSE
Levy-w	0.042	deVries-w	0.045	deVries-w	0.049	deVries-wi_{GMM}	0.057
Gori-vphf-w	0.042	deVries-wi_{GMM}	0.052	Masch-⊥-$fib_{\|}$	0.057	Levy-$wi_{\|}$	0.065
GeoMean-s_{GMM}	0.042	Masch-⊥-$fib_{\|}$	0.055	Levy-$wi_{\|}$	0.059	Levy-i-$d_{\|}$	0.068
deVries-w	0.043	Masch-⊥-fib_{GMM}	0.058	deVries-wi_{GMM}	0.060	EMT-s_{GMM}	0.068
deVries-f	0.045	Maxwell-wi_{GMM}	0.059	Levy-i-d_{GMM}	0.064	Masch-‖-$fib_{\sum}$	0.069
EMT-s_{GMM}	0.046	EMT-s_{GMM}	0.062	Gori-vphf-wi	0.064	Masch-‖-fib_{GMM}	0.069
Maxwell-w	0.046	Levy-i-d_{GMM}	0.065	Masch-⊥-fib_{GMM}	0.071	deVries-w	0.072
Levy-f-$d_{\|}$	0.047	Levy-$wi_{\|}$	0.065	Masch-‖-fib_{GMM}	0.072	Gori-vphf-wi	0.073
Masch-⊥-fib_{GMM}	0.051	Gori-vphf-wi	0.066	EMT-s_{GMM}	0.072	Maxwell-wi_{GMM}	0.074
Gori-hpi-w	0.053	Masch-‖-fib_{GMM}	0.066	deVries-i	0.073	Masch-⊥-$fib_{\|}$	0.080

λ_{wi}. Consequently, the k_j must be evaluated individually for each meat having different initial water content. Evaluation of λ_{wi} by the GMM model appears to be beneficial to deVries and Maxwell model, while the ‖ model works better for Levy model. The use of *w* as the continuous medium is beneficial only to deVries model, particularly from −1 to −20 °C. The use of *fat* as the continuous medium is beneficial only to foods with high fat content.

Overall, relatively small differences in predictions were observed between the best model versions by *deVries*, *Levy*, *Mascheroni*, *Maxwell* or *Gori* as applied to frozen meats with high water content. These differences could also be generated by uncertainty in food composition, temperature independent thermal conductivity of ice, measurement errors, and limitation of predictive models. The above results are preliminary and need to be confirmed by testing the models against the experimental data representing a wider variety of frozen foods. In addition, it would be beneficial to investigate the influence of temperature dependent thermal conductivity of all food components on the predictive model performance.

Acknowledgements

The authors wish to express their appreciation to Saint Mary's University in Canada, University of Rome-Tor Vergata, and Agenzia Spaziale Italiana for providing funds to complete this study. Acknowledgment is given to Mr Jeff Levy for his contribution to initial development of Excel simulations.

References

[1] A. Eucken, Allgemeine Gesetzmassigkeiten fur das Warmeleitvermogen verschiedener Stoffarten und Aggregatzustande, Forschung und Gebiete Ingenieur (Ausgabbe A) 11 (6) (1940).

[2] F.L. Levy, A modified Maxwell–Eucken equation for calculating the thermal conductivity of two-component solutions or mixtures, Int J Refrigeration 4 (1981) 223–225.

[3] M. Mattea, M.J. Urbicain, E. Rotstein, Prediction of thermal conductivity of vegetable foods by the effective medium theory, J Food Sci 51 (1) (1986) 113–115 [see also p. 134].

[4] R.H. Mascheroni, J. Ottino, A. Calvelo, A model for the thermal conductivity of frozen meat, Meat Sci 1 (1977) 235–243.

[5] Q.T. Pham, in: W.E.L. Spiess, H. Schubert (Eds.), Prediction of thermal conductivity of meats and other animal products from composition data, Engineering and Food vol. 1, Elsevier Applied Science, London, 1990, pp. 408–423.

[6] D.A. DeVries, Thermal properties of soils in: W.R. van Wijk (Ed.), Physics of plant environment, Wiley, New York, 1963, pp. 210–235.

[7] F. Gori, A theoretical model for predicting the effective thermal conductivity of unsaturated frozen soils, Proceedings of the fourth international conference on Permafrost, Fairbanks (Alaska), National Academy Press, Washington, DC, 1983. p. 363–368.

[8] J. Sundberg, Thermal properties of soils and rocks. Chalmers University of Technology and University of Gothenburg, Goteborg, Sweden. PhD Thesis; 1988, p. 1–310.

[9] K. Lichtenecker, Dielectric constant of natural and synthetic mixtures, Zeitschrift fur Physik 27 (1926) 115–158.

[10] O. Johansen, Thermal conductivity of soils. Trondheim, Norway, PhD Thesis; 1975 (CRREL translation 637, 1977).

[11] R. McGaw, Heat conduction in saturated granular materials. In: Effects of temperature and heat on engineering behavior of soils. Highway research board special report; 1969, vol. 103, p. 114–31.

[12] H. Fricke, The electrical conductivity of a suspension of homogeneous spheroids, Phys Rev 24 (1924) 575.

[13] H.S. Carslaw, J.C. Jaeger, Conduction of heat in solids, 2nd ed, Oxford University Press, Oxford, 1986.

[14] D.A.G. Bruggeman, Dielectric constant and conductivity of mixtures of isotopic materials (in German), Ann Phys 24 (1935) 636–679.

[15] R. Landeauer, The electrical resistance of binary metallic mixtures, J Appl Phys 23 (1952) 779–784.

[16] D.J. Cleland, K.J. Valentas, Prediction of freezing time and design of food freezers in: R.P. Singh, K.J. Valentas (Eds.), Handbook of food engineering practice, CRC Press, Boca Raton, Florida, 1997, pp. 71–124.

[17] Q.T. Pham, J. Willix, Thermal conductivity of fresh lamb meat, offals and fat in the range −40 − +30 °C: measurements and correlations, J Food Sci 54 (3) (1989) 508–515.
[18] Y. Choi, M.R. Okos, Effects of temperature and composition on the thermal properties of foods in: M. Le Maguer, P. Jelen (Eds.), Food engineering and processes applications, transport phenomena, Elsevier Applied Science, Amsterdam, 1986, pp. 93–101.
[19] H.G. Schwartzberg, Effective heat capacity for the freezing and thawing of food, J Food Sci 41 (1976) 152–156.